Modeling and Verification of Molten Compound with Barium Sulfate Particles

Mari Niemelä[1], Jorma Roine[2], Johanna Aho[2], Markus Hannula[1], Ilari Jönkkäri[1], Jari Hyttinen[1] and Minna Kellomäki[1]

[1]Tampere University, FI-33720 Tampere, Finland
[2]Bayer Oy, Research & Development, Pharmaceuticals, CPD-DDI-Drug Carrier & Depot Systems, FI-20210 Turku, Finland

ABSTRACT

Polymers and polymeric compounds with filler particles are typically processed using extrusion or injection molding. To save resources when designing these processes and to minimize the required experiments, numerical simulations could be applied. For high quality simulations, the accuracy of the applied material properties is one important aspect. Therefore, the aim of this study was to model three important material properties for a molten compound based on the properties of its polymer matrix and filler particles. In addition, the modeled properties were verified with the measured ones.

The studied material properties were the viscosity, thermal conductivity, and specific heat capacity. The viscosity was modelled using the relative viscosity according to Maron-Pierce and Carreau-Yasuda model parameters for the polymer, but this model underestimated the viscosity. The thermal conductivity was modelled using Hasselman's model. The challenge of this model was that it required a parameter (interfacial thermal conductance) which was not found from literature nor measured. When a value fitted to measurement was applied for the conductance, the model predicted the measured data well. The specific heat capacity was modeled using the weighted average of the conductance for the polymer and filler and the model corresponded with the measured data well.

INTRODUCTION

Polymers and polymeric compounds with filler particles are typically processed using extrusion or injection molding. These processes are often designed based on experiments which consume resources. To minimize the required experiments, numerical simulations could be applied. For high quality simulations, the accuracy of the applied material properties is one important aspect.

The aim of this study was to model the material properties of a molten compound based on the properties of its polymer matrix and filler particles. The modelled properties were verified with the measured ones. Especially, the model parameters for the compound including barium sulphate filler particles were studied since they were limited in literature. The measured and modelled material properties were the viscosity (η), thermal conductivity (k), and specific heat capacity (C_p). In addition, the filler particle size distribution in the pellets and during injection molding was studied as well as its effect on the viscosity and thermal conductivity of the compound.

MATERIALS

The studied polymer was a semi-crystalline low-density polyethylene (LD-PE) and two polymer batches were used (B1 and B2). The filler was a synthetic barium sulfate ($BaSO_4$) with the mean particle diameter of 1 μm and one filler batch was applied (F). The compound pellets were mixed with a Farrel continuous mixer using two LD-PE batches (B1 and B2) and one $BaSO_4$ batch to produce two compound batches (cB1 and cB2). The nominal mass fraction of the filler particles in the compounds was 22 w-% which corresponded approximately to volume fraction $\phi = 0.047$ when the densities of the polymer**Feil! Fant ikke referansekilden.** and filler were 763 kg/m^3 and 4400 kg/m^3, respectively. For each compound batch (cB1 and cB2), two samples (A and C) were extracted for material testing. In addition, the compound batch samples were also processed with a small injection molding machine to study the particle size evolution in processing.

EXPERIMENTAL METHODS

The filler particle size was evaluated for four compound samples (cB1/A, cB1/C, cB2/A, and cB2/C) using micro computed tomography (μ-CT). The samples were imaged with MicroXCT-400. The source voltage was 80 kV and the current was 125 μA. 1601 projections were taken with 2 seconds exposure time. The reconstructed image stack had a voxel size of 5,64 μm. Visualizations and analysis were completed with the Avizo 2022.1 software. Image stacks were thresholded manually and the particles' volumes and equivalent diameters were calculated with the Label analysis function.

The samples for the particle size evaluation were obtained from the compounded pellets but also from three functional zones of the injection molding machine (feed, compression, and metering zones). The samples from the functional zones were collected during a screw pull-out test. In this test, 20 injections were first run to stabilize the molding cycle. Then, the screw was stopped at its back position and removed from the machine while the barrel heaters were still on. Finally, the samples were carefully obtained from approximately the middle of the functional zones using a scalpel.

The viscosity (η) was measured using parallel-plate oscillatory rheometer over frequency range of 0.126-512 rad/s. The polymer batches B1 and B2 as well as compound batch samples cB1/C and cB2/A were tested. The tests were conducted at three different temperatures (180°C, 190°C and 200°C) using three parallel samples. Additional oscillatory and rotational tests were conducted to estimate the relation between the complex viscosity and the shear viscosity. These tests were done at temperatures 180°C, 190°C and 200°C for the polymer batch B2 and the compound batch sample cB2/A. One measurement for each data point was conducted.

The thermal conductivity (k) was measured at 190°C using polymer batches B1 and B2 and compound batch samples cB1/C and cB2/A. During the measurements, the material was melted in a capillary rheometer, a thermal conductivity probe was set in the rheometer and after stabilization, five parallel measurements were conducted.

The specific heat capacity (C_p) was determined using differential scanning calorimeter (DSC). The tested samples for polymer, filler and compound were B2, F and cB2/A, respectively. The samples were first heated to 160°C for 5 min at the rate of 10°C/min and cooled back to room temperature to minimize the influence of their thermal history. The analysis run started with a 2 min isotherm, followed by the temperature scan done at the heating rate of 10 °C/min and ended in a 5 min isotherm. Four parallel samples were tested.

MODELING METHODS

Viscosity

The polymer η was modelled using Carreau-Yasuda model and its temperature dependency using Arrhenius law as follows[Feil! Fant ikke referansekilden.]

$$\eta = a_T \cdot \eta_0[1 + (a_T \cdot \lambda\dot{\gamma})^a]^{\frac{(n-1)}{a}} \quad (1)$$

$$a_T = exp\left[\frac{E}{R}\left(\frac{1}{T} - \frac{1}{T_{ref}}\right)\right] \quad (2)$$

where η_0 is the zero shear rate viscosity, λ is the time constant, n is the power law exponent and a is the dimensionless parameter defining the transition from the Newtonian range to the non-Newtonian range of the viscosity. For the temperature shift parameter (a_T), E is the activation energy of the polymer, R is the gas constant and T_{ref} is the reference temperature.

The compound η is typically modelled using the relative viscosity (η_r) defined as the ratio of the compound viscosity to the polymer matrix viscosity[Feil! Fant ikke referansekilden.]. The η_r models are often dependent on the filler volume fraction (ϕ) as well as the maximum packing fraction (ϕ_m) which is related to the arrangement, shape, and size distribution of the particles[Feil! Fant ikke referansekilden.]. In this work, η_r was predicted using the models in **Table 1** and $\phi_m = 0.37$ for random close packing of agglomerated particles.

TABLE 1: Models for the relative viscosity ($\eta_r = \eta_{compound} / \eta_{polymer}$).

Model	Equation	Notes
Batchelor[Feil! Fant ikke referansekilden.]	$\eta_r = 1 + 2.5\phi + k\phi^2$ (3)	For dilute compounds (ϕ few %) k = 5.2 applied for non-colloidal particles
Thomas[Feil! Fant ikke referansekilden.]	$\eta_r = 1 + 2.5\phi + 10.05\phi^2 + A\,exp(B\phi)$ (4)	For monodispersed, spherical particles with empirical parameters A = 0.00273 and B = 16.6
Maron-Pierce[Feil! Fant ikke referansekilden.]	$\eta_r = \left(1 - \frac{\phi}{\phi_m}\right)^{-2}$ (5)	Model recommended for irregular particles and fibers[Feil! Fant ikke referansekilden.]
Frankel-Acrivos[Feil! Fant ikke referansekilden.]	$\eta_r = \frac{9}{8}\left[\frac{\left(\frac{\phi}{\phi_m}\right)^{1/3}}{1 - \left(\frac{\phi}{\phi_m}\right)^{1/3}}\right]$ (6)	Model recommended for spherical or nearly spherical particles[Feil! Fant ikke referansekilden.]
Mooney[Feil! Fant ikke referansekilden.]	$\eta_r = exp\left(\frac{2.5\phi}{1 - K\phi}\right)$ (7)	K empirical parameter (1.35…1.91) K estimated as $1/\phi_m$

Thermal conductivity

Two models predicting the effective compound k were estimated. First, Maxwell-Eucken's model was applied. This model assumes that the homogeneous spherical particles are dispersed randomly into the matrix, and they do not interact. Maxwell-Eucken's model is defined as follows[Feil! Fant ikke referansekilden.]

$$k = k_p \frac{2k_p + k_f + 2\phi(k_f - k_p)}{2k_p + k_f - \phi(k_f - k_p)} \tag{8}$$

where k_p is the thermal conductivity of the polymer, k_f is the thermal conductivity of the filler and ϕ is the filler volume fraction. Second, Hasselman's model was applied. This model assumes also that the spherical, randomly dispersed particles but it considers also the interfacial thermal barrier between the polymer and filler.[Feil! Fant ikke referansekilden.] Hasselman's model is determined as follows[Feil! Fant ikke referansekilden.]

$$k = k_p \frac{2\left(\frac{k_f}{k_p} - \frac{k_f}{ah_c} - 1\right)\phi + \frac{k_f}{k_p} + \frac{2k_f}{ah_c} + 2}{\left(1 - \frac{k_f}{k_p} + \frac{k_f}{ah_c}\right)\phi + \frac{k_f}{k_p} + \frac{2k_f}{ah_c} + 2} \tag{9}$$

where k_p is the thermal conductivity of the polymer, k_f is the thermal conductivity of the filler, ϕ is the filler volume fraction, a is the filler radius and h_c is the boundary conductance.

Specific heat capacity

The polymer C_p and filler C_p are typically dependent on temperature[Feil! Fant ikke referansekilden.]. In this study, a linear temperature dependent fit was applied for both polymer $(C_{p,p})$ and filler $(C_{p,f})$ as follows

$$C_{p,p} = c_{slope,p} * T + c_{intercept,p} \tag{10}$$

$$C_{p,f} = c_{slope,f} * T + c_{intercept,f} \tag{11}$$

where T is the temperature, $c_{slope,i}$ is the slope and $c_{intercept,i}$ is the interception point of the linear fit. The compound C_p was modelled using the weighted average as follows

$$C_p = C_{p,p} + m_f(C_{p,f} - C_{p,p}) \tag{12}$$

where $C_{p,p}$ is the specific heat capacity of polymer, $C_{p,f}$ is the specific heat capacity of the filler and m_f is the mass fraction of the filler.

RESULTS AND DISCUSSION

Particle size

The mean and median equivalent diameters of the particles in the pellets as well as in the functional zones of the injection molding process are presented in **Figure 1** for the compound batches cB1 and cB2. The number mean D[1,0] and median D50 for both batches were constants during the process and no deviations between the batches were detected. On the contrary, the volume mean D[4,3] and median Dv50 showed some deviation between the compound batches. The deviation was partly caused by the small size of the studied samples from the functional zones since the sporadic large agglomerates (the equivalent diameters up to 300 µm) affected significantly D[4,3] and Dv50 but some large agglomerates could have been undetected due to the studied sample size. Generally, no pattern for the particle size evolution was detected during the process. Therefore, it was assumed that the size distribution did not change significantly during the process and that the material properties measured using the pellets described accurately enough the material properties during the process.

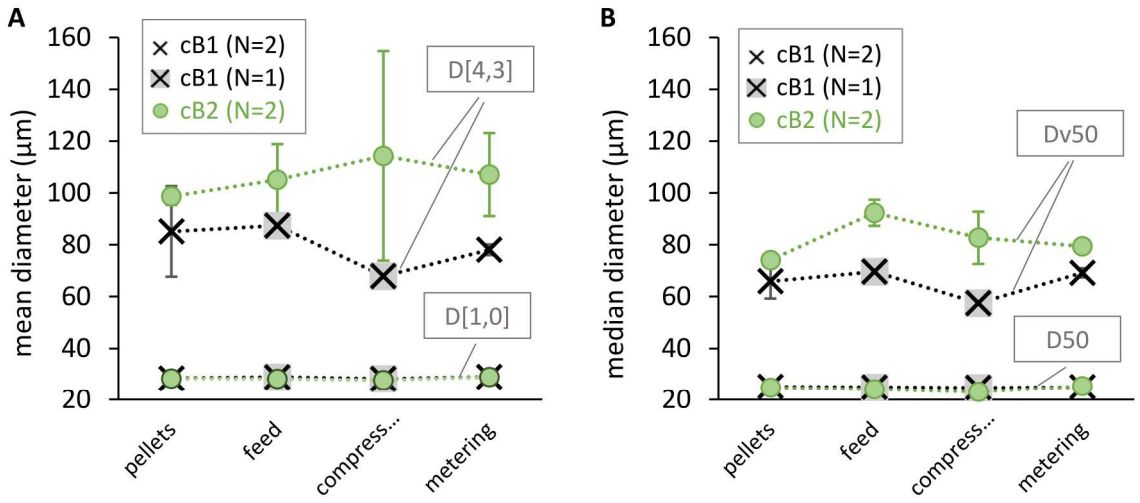

FIGURE 1: A – the number D[1,0] and volume means D[4,3] of the equivalent particle diameters for the compounds cB1 and cB2 in the pellets as well as in the feed, compression and metering zones of the injection molding machine. The values are presented as the mean of the samples A and C for each compound and the error bars indicate SD (N=2, except for cB1 in the feed and compression zones N=1). **B** – the number D50 and volume Dv50 medians similarly to figure A.

Viscosity

The measured η of the polymer batches (B1 and B2) were similar while some deviation was noticed between the compound batch samples (cB1/C and cB2/A) especially at the low angular frequencies (results not shown here). However, the deviation was within the method uncertainty of 5% and thus, the slightly different particle size distribution in the compounds did not significantly affect the viscosity. Same assumption was made by Metzner**Feil! Fant ikke referansekilden.** who stated that the particle size distribution has little effect on the compound viscosity when the filler volume fraction is less than 0.20.

For the polymer, Carreau-Yasuda model was fitted to the measured datapoints (means of batches B1 and B2, N=6) using the ordinary least squares method to minimize the sum of squared residuals and they corresponded well with the measured data. The fitted parameters for Carreau-Yasuda model were η_0 = 15 013 Pas, λ = 1.81 s, n = 0.37, a = 0.46 and E = 48 148 J/mol while T_{ref} was 190°C.

For the compound, the measured η is presented with markers in **Figure 2A** (means of batches cB1/C and cB2/A, N=6) and as expected, the compound η was higher than the

corresponding polymer η. The modelled η was predicted using the fitted parameters of the polymer η and the relative viscosity (η_r). The η_r calculated from measurements is presented with markers in **Figure 2B** and as expected, the particles have higher effect on the viscosity at the low angular frequency than at the high angular frequency. The effect also increased when temperature increased. The modelled η_r was calculated using the models in **Table 1,** $\phi = 0.047$ and $\phi_m = 0.37$. The models according to Batchelor and Frankel-Arcivos predicted that $\eta_r = 1.13$ while the models by Thomas and Mooney estimated $\eta_r = 1.14$. Maron-Pierce model had the estimation closest to the measured data ($\eta_r = 1.31$) and it was selected to predict the compound η. The modelled η at the different temperatures are presented with lines in **Figure 2A.** They underestimated the compound η and corresponded poorly with the measured data since the modelled η_r did not consider the temperature and angular frequency dependencies of the measured η_r.

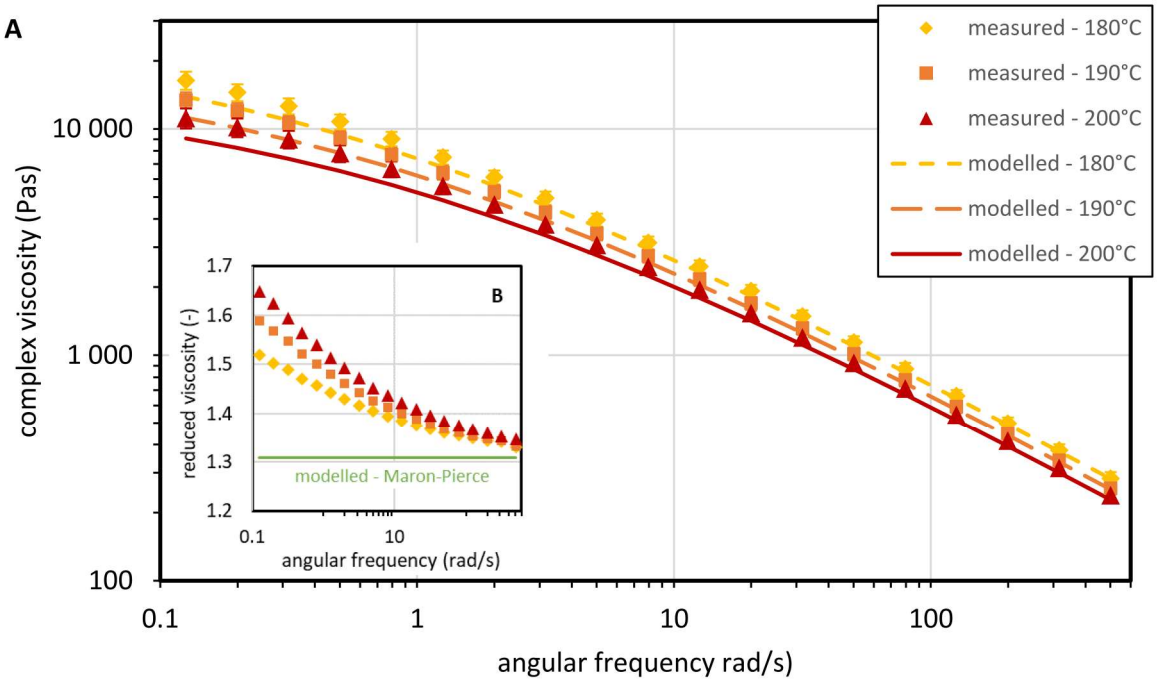

FIGURE 2: A – The compound η at three temperatures: The measured datapoints (markers) were calculated as the mean of the compound batch samples (cB1/C and cB2/A). The error bars are included and describe SD (N=6) and the 5% measurement method error. The modelled η (lines) were obtained using the Carreau-Yasuda parameters for the polymer and the η_r according to Maron-Pierce model. **B** – The η_r at three temperatures: the measured datapoints (markers) were calculated as the ratio of the compound η (mean of cB1/C and cB2/A, N=6) to the polymer η (mean of B1 and B2, N=6). The modelled η_r (line) was according to Maron-Pierce model ($\phi = 0.047$ and $\phi_m = 0.37$).

The relation between the complex η and the shear η typically applied for simulations was also studied. According to the empirical Cox-Merz rule, the complex η as the function of the angular frequency equals to the shear η as the function of the shear rate. However, this rule might not apply for all polymers and compounds with filler particles[Feil! Fant ikke referansekilden.]. The complex η measured in oscillatory mode and the shear η measured in rotational mode were compared (results not shown here) and some deviation was observed between the different measurement modes for both polymer and compound. This implied that Cox-Merz rule is not applicable for the LD-PE and LD-PE + $BaSO_4$ compounds studied in this work. However, only

one measurement for each data point was conducted and thus, further testing should be done to conform this assumption.

Thermal conductivity

The measured k for the different polymer batches (B1 and B2) as well as the compound batch samples (cB1/C and cB2/A) did not differ considerably: Thus, it was assumed that the different particle size distribution in the compounds did not significantly affect k and the polymer k was calculated as the mean of the two batches (N=10). Similar procedure was applied for the compound. As a result, the measured k for the polymer and compound were 0.269 ± 0.005 W/(mK) and 0.255 ± 0.005 W/(mK), respectively. The measured compound k is presented in **Figure 3A**. Note that the thermal conductivity was not measured as a function of the particle diameter.

The modelled compound k predicted by Maxwell-Eucken's model was 0.294 W/(mK) which did not correspond to the measured data. The other applied model was Hasselman's model which required the interfacial thermal conductance (h_c). No data of the conductance for the studied compound was measured or found from literature and thus, arbitrary values for h_c ranging between 10 – 2 000 W/m^{2}K were applied. Using these hc values, Hasselman's model corresponded well with the measured data as presented in **Figure 3A** (dashed lines).

Specific heat capacity

The measured C_p for polymer (batch B2), filler (batch F) and compound (batch sample cB2/A) are presented in **Figure 3B** with markers as the mean of the measured data (N=4). The fitted C_p for the polymer and filler are presented with the dashed lines. The slope and the interception point of the linear fit for the polymer C_p were 0.0031 J/(g°C^2) and 2.14 J/(g°C), respectively and for the filler C_p 0.0003 J/(g°C^2) and 0.49 J/(g°C), respectively. The fitted values corresponded well with the measured data. For the compound, the modelled C_p predicted using the weighted average is presented in **Figure 3B** with the solid line and it corresponded also well with the measured data.

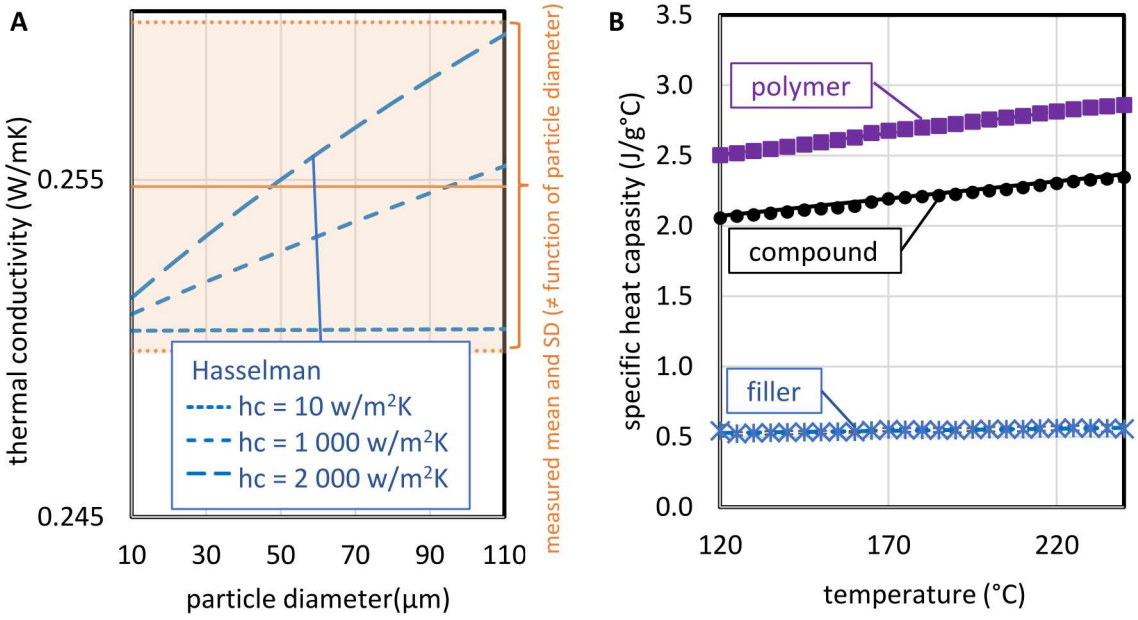

FIGURE 3: A - The compound k at 190°C: The measured k (solid line) was calculated as the mean of the compound batch samples cB1/C and cB2/A and the error as SD (N=10). The modelled k (dashed

lines) was obtained from Hasselman's model using several interfacial conductance (h_c). **B** – Cp: The measured Cp (markers) were calculated as the means of the four parallel measurements (polymer B2, filler F and compound cB2/A). The error bars are included and describe SD (N=4). The fitted Cp (dashed lines) for polymer and filler were obtained by fitting the linear regressions to the measured data and the modelled compound Cp (solid line) by applying the weighted average.

CONCLUSIONS

The studied material properties were the viscosity, thermal conductivity, and specific heat capacity. The viscosity of the compound was modelled using the relative viscosity according to Maron-Pierce model as well as the Carreau-Yasuda parameters for the polymer. However, this model underestimated the compound viscosity and it corresponded poorly to the measured data since the applied relative viscosity did not consider the effect of the temperature and angular frequency. In addition, estimating the shear viscosity from the complex viscosity according to the empirical Cox-Merz rule might not be applicable for the studied materials, but additional experiments are needed to confirm this conclusion. The thermal conductivity was modelled using Hasselman's model. The challenge of this model was that it required a parameter (interfacial thermal conductance) which was not found from literature nor measured. When a value fitted to the measurements was applied for the parameter, the model predicted well the measured data. The specific heat capacity was modeled using the weighted average of the specific heat capacities for the polymer and filler and the model corresponded well with the measured data. In addition, the filler particle size distribution was studied and no pattern for the particle size evolution during the process was detected. Therefore, it was assumed that the distribution did not change significantly during the process and that the material properties measured using the pellets described accurately enough the material properties during the process. The particle size distribution had no effect on the viscosity and thermal conductivity of the compound.

Acknowledgements: The authors would like to thank Taina Tjäder and Riku Sundell (Bayer oy, Turku, Finland) for their contribution.

REFERENCES

1. Tadmor, Z.; Gogos, C. G. *Principles of Polymer Processing*, 2nd ed.; John Wiley & Sons, Inc., 2006.
2. Wilczyński,K. *Rheology in Polymer Processing: Modeling and Simulation*; Hanser, 2021.
3. Metzner, A. B. Rheology of Suspensions in Polymeric Liquids. *J. Rheol*. **1985**, *29*(6), 739-775. DOI: 10.1122/1.549808.
4. Javanbakht, Z. Computational Modelling of Fiber-Reinforced Composites and Nanocomposites. Ph.D. Dissertation, Griffith University, Queensland, Australia, 2019. https://doi.org/10.25904/1912/187 (accessed 2023-1-20).
5. Agassant, J-F.; Avenas, P.; Carreau, P. J.; et al.. *Polymer Processing: Principles and Modeling*, 2nd ed.; Hanser, 2017.
6. Kataoka, T.; Kitano, T.; Sasahara, M.; Nishijima, K. Viscosity of particle filled polymer melts. *Rheol. Acta* **1978**, *17*(2), 149–155. DOI:10.1007/bf01517705.
7. Shen, M.; Cui Y.; He, J.; Zhang, Y. Thermal conductivity model of filled polymer composites. *Int. J. Miner. Metall.* **2011**, *18*(5), 623-631. DOI: 10.1007/s12613-011-0487-9.
8. Hasselman D.P.H.; Johnson, L. F. Effective Thermal Conductivity of Composites with Interfacial Thermal Barrier Resistance. *J. Compos. Mater.* **1987**, *21*(6), 508-515. DOI:10.1177/002199838702100602.